Muon capture on ^{35}Cl

S. Arole,[1] D. S. Armstrong,[2] T. P. Gorringe,[1] M. D. Hasinoff,[3] M. A. Kovash,[1] V. Kuzmin,[4]
B. A. Moftah,[3,*] R. Sedlar,[1,†] T. J. Stocki,[3,‡] and T. Tetereva[5]
[1]*Department of Physics and Astronomy, University of Kentucky, Lexington, Kentucky 40506*
[2]*Department of Physics, College of William and Mary, Williamsburg, Virginia 23187*
[3]*Department of Physics and Astronomy, University of British Columbia, Vancouver, British Columbia, Canada V6T 1Z1*
[4]*Bogoliubov Laboratory of Theoretical Physics, Joint Institute for Nuclear Research, Dubna 141 980, Russia*
[5]*Dubna Branch of Skobeltsyn Institute of Nuclear Physics, Lomonosov Moscow State University, Dubna 141 980, Russia*
(Received 25 April 2002; published 10 December 2002)

We report measurements of γ-ray spectra from muon capture on ^{35}Cl. For the allowed Gamow-Teller transitions to the ^{35}S(2939,3/2$^+$) state and the ^{35}S(3421,5/2$^+$) state we obtained their capture rates, hyperfine dependences, and $\gamma-\nu$ correlation coefficients. The capture rates and hyperfine dependences were compared to shell model calculations using the complete $1s-0d$ space and the universal SD interaction. With $g_p/g_a = 6.7$ and $g_a = -1.00$ (or $g_a = -1.26$) we found agreement of the model and the data at the 1–2 σ level. However, we caution that the transitions are sensitive to $l=2$ forbidden matrix elements.

DOI: 10.1103/PhysRevC.66.065501 PACS number(s): 23.40.Hc, 27.30.+t

I. INTRODUCTION

The induced pseudoscalar coupling (g_p) is the least known of the proton's weak couplings. For the free proton, the coupling's determination is an important test of chiral symmetry breaking [1–3]. For the bound proton, the coupling's renormalization is sensitive to π exchange currents, Δ-hole excitations and possible precursor effects of chiral phase transitions in hot, dense nuclear matter [4–6].

Unfortunately the effects of g_p are subtle and elusive. In few-body systems recent results from radiative muon capture (RMC) on ^{1}H [7,8] and ordinary muon capture (OMC) on ^{3}He [9] are available. However their interpretations are complicated by muon chemistry in ^{1}H and two-body currents in ^{3}He, and the puzzling discrepancy between the values of g_p from RMC on ^{1}H and OMC on ^{3}He is so far unexplained. In complex nuclei new results from allowed transitions on ^{11}B [10], ^{23}Na [11], and ^{28}Si [12–14] are also available. In nuclei the difficulty is disentangling the weak dynamics from nuclear structure. The majority of data on nuclei are consistent with an unrenormalized g_p, but more experiments on other transitions would be interesting.

In this article we report measurements of γ-ray spectra from muon capture on ^{35}Cl. In particular we describe the determination of capture rates, hyperfine dependences and $\gamma-\nu$ angular correlations for two ^{35}Cl$\rightarrow^{35}$S allowed Gamow-Teller transitions. We also compare their capture rates and hyperfine dependences to a large basis shell model calculation, and discuss their sensitivity to the weak couplings and the nuclear structure.

The paper is organized as follows. In Secs. II and III we describe the measurement setup and experimental results. In Sec. IV we discuss the comparison of the model and the data, and the sensitivity to the couplings constants and the nuclear model. We conclude in Sec. V.

II. EXPERIMENTAL SETUP

The experiment was conducted using the M9B backward decay muon beamline at the TRIUMF cyclotron. The setup was similar to our earlier studies of other $1s-0d$ shell nuclei (see Refs. [11,13,15]).

We employed a μ^- beam of incident momentum 60 MeV/c, stopping rate 1.2×10^5 s^{-1}, and e and π contamination of 10% and $\leqslant$0.1%. Muon stops were counted in a plastic scintillator beam telescope comprising two counters ($S1$ and $S2$) upstream of the target and one counter ($S3$) downstream of the target. The target material was isotopically enriched Na^{35}Cl (99% chlorine-35) powder of mass 50 g [we used isotopically pure chlorine-35 to avoid γ-ray backgrounds from ^{37}Cl(μ,2nν) reactions]. The material was packed in a thin-walled, disk-shaped, polyethylene container. The target was viewed by a HPGe detector with an in-beam energy resolution of 2.2 keV (full width at half maximum) and in-beam time resolution of 10 ns (FWHM) for 1.33 MeV ^{60}Co γ-rays. A segmented NaI annulus, surrounding the HPGe detector, was used to suppress the Compton scattering background. A second NaI array, viewing the Na^{35}Cl target, was used for collection of γ-ray coincidence data.

Events were digitized on fulfillment of the logic condition $Ge\cdot\overline{CS}\cdot\mu STOP\cdot\overline{busy}$, where Ge indicates a signal in the HPGe detector, $\overline{CS}$ indicates no signal in the NaI suppressor, $\mu STOP$ indicates a μ^- stop in the preceding 2.0 μs, and $\overline{busy}$ indicates that the acquisition is live. For each event we recorded energy and timing signals from the Ge detector, NaI arrays, and beam counters. We also recorded a multihit time history of muon stops, and a pile-up bit and an overload bit

*Present address: Department of Oncology, King Faisal Specialist Hospital and Research Center, Jeddah 21499, Saudi Arabia.
†Present address: The Boeing Company, Denver Engineering Center, 14261 E. 4th Ave., MC AG-00 Bldg 6 Suite 100, Aurora, CO 80011.
‡Present address: Communications Research Center, 3701 Carling Ave., Box 11490, Station H, Ottawa, Ontario, Canada K2H 8S2.

TABLE I. γ-ray yields per μCl atom formed for the cleanly identified lines from $^{35}\mathrm{Cl}(\mu,\nu)^{35}\mathrm{S}$. Columns 1–5 give the relevant energies, lifetimes, and branching ratios from Ref. [20]. The coincident fraction f_c is discussed in Sec. III D.

E_γ (keV)	$(E,J^\pi)_i$ (keV)	$(E,J^\pi)_f$ (keV)	BR (%)	Lifetime	γ-ray yield (per μCl atom)	coinc. frac. f_c
1991.3	$(1991,7/2^-)$	$(0,3/2^+)$	100	(1.02 ± 0.05) ns	$(7.1\pm1.2)\times10^{-3}$	1.27 ± 0.06
2347.8	$(2348,3/2^-)$	$(0,3/2^+)$	75	0.89 ± 0.12 fs	$(2.8\pm0.5)\times10^{-3}$	0.77 ± 0.15
2717.1	$(2717,5/2^+)$	$(0,3/2^+)$	94	(70 ± 25) fs	$(2.9\pm0.5)\times10^{-3}$	1.00 ± 0.39
2939.6	$(2939,3/2^+)$	$(0,3/2^+)$	100		$(5.4\pm0.9)\times10^{-3}$	<0.30
3421.0	$(3421,5/2^+)$	$(0,3/2^+)$	100	<70 fs	$(5.3\pm0.9)\times10^{-3}$	0.10 ± 0.15

from the HPGe. The pile-up bit identifies events with a preceding Ge detector hit within 50 μs and the overload bit identifies events with a preceding >10 MeV Ge detector hit within 500 μs (for details see Ref. [11]). Data were collected for 4.2×10^{10} muon stops in the $Na^{35}Cl$ target, along with γ-ray background data from a LiCl target and x-ray calibration data from various materials.

Offline the data were sorted into histograms corresponding to (i) a HPGe singles γ-ray energy spectra, (ii) a HPGe·NaI coincidence γ-ray energy spectra (i.e., a HPGe energy spectrum with a NaI coincidence requirement), and (iii) many HPGe·$\mu STOP$ time-binned γ-ray energy spectra (i.e., HPGe energy spectra corresponding to different time bins). The time bins were defined by the time difference between the incoming muon and the outgoing γ-ray. In filling the histograms we rejected any events with either an overload signal or a pile-up signal in the HPGe.

III. EXPERIMENTAL RESULTS

A. HPGe calibration

A large body of muonic x-ray data was collected in order to determine the HPGe photon acceptance, energy resolution, and time resolution. The data comprised *K*, *L*, and *M* series x-ray spectra from S, Ca, In, Nb, Fe, Pb, and Bi, and spanned a range of energies from 500 to 4000 keV.

To determine the acceptance with muonic x-rays we either (i) used published yield data for individual x-rays [16–19] or (ii) assumed a yield of unity for the entire *K*-series. Then we performed a least squares fit of the measured acceptances to a smooth empirical curve to permit interpolation to the interesting γ-ray energies.

For the energy resolution determination we fit the numerous x-ray peaks to a central Gaussian supplemented by both low and high energy tails. The width of the central Gaussian was observed to increase from 2.2 keV at 1000 keV to 3.6 keV at 3000 keV. Both low energy and high energy tails were observed, but their effects on the fits to the ^{35}S γ-rays were almost negligible (see Sec. III G). The best fit values of the line shape parameters were used to fix the instrumental line shape in the least squares fits to the γ-ray data.

For the time resolution determination we fit the prompt peaks of the x-ray lines with a central Gaussian supplemented by both early and late tails (energy windows were used to select the x-rays). We found that, for photon energies above 1000 keV, the Gaussian width was approximately constant at 10 ns FWHM, but the resolution rapidly got worse for lower energies. A weak tail at late times was observed, but its effect on the fits to the ^{35}S γ-rays was almost negligible (see Sec. III F). Again, the best fit values of the line shape parameters were used to fix the line shape in the least squares fits to the γ-ray data.

More details on the procedures for the determination of the photon acceptance, energy resolution, and time resolution can be found in the Refs. [11,15].

B. Line identification

About 80 peaks were found in the γ-ray spectrum from muon stops in $Na^{35}Cl$. To match the peaks to known γ-ray lines we searched the nuclear γ-ray database at the National Nuclear Data Center (NNDC) [20] for all isotopes corresponding to the capture reactions $^{23}\mathrm{Na}(\mu^-,xpyn\,\nu)$ and $^{35}\mathrm{Cl}(\mu^-,xpyn\,\nu)$ where $x,y=0,1,2$. For conclusive identification we demanded (i) an energy match within experimental uncertainties, (ii) consistency with other γ-branches of the parent state, and (iii) Doppler broadening if the parent state lifetime was less than the recoil stopping time. This procedure yielded five γ-rays from levels in ^{35}S, 21 γ-rays from levels in ^{34}S, and four γ-rays from levels in ^{33}S.

The conclusively identified γ-rays from ^{35}S are listed in Table I and shown in Fig. 1. The five γ-rays all feed the ^{35}S ground state and correspond to three allowed transitions to the $(2717,5/2^+)$, $(2939,3/2^+)$, and $(3421,5/2^+)$ states and two forbidden transitions to the $(1991,7/2^-)$ and $(2439,3/2^-)$ states.

In addition, the production of γ-rays from the $^{35}\mathrm{S}(1572,1/2^+)$ and $^{35}\mathrm{S}(4028,1/2^+-5/2^+)$ levels is possible. For the $(1572,1/2^+)$ level, a γ-peak was clearly identified at 1572 keV, but unfortunately it matches the energies of both the $1572\rightarrow0$ ^{35}S transition and a $4877\rightarrow3304$ ^{34}S transition. The observed 1572 keV peak is Doppler broadened, and indicates that the short lifetime ^{34}S state is the major γ-ray source, but some contribution from the $^{35}\mathrm{S}(1572,1/2^+)$ level is a possibility. For the $(4028,1/2^+-5/2^+)$ level, weak lines were identified at energies of ~5 keV below that expected for $4028\rightarrow1572$, $4028\rightarrow2348$, and $4028\rightarrow2939$ transitions. Note the experimental uncertainty for the 4028 keV excitation energy is about ±2 keV [20], so these peaks in the $Na^{35}Cl$ data may be

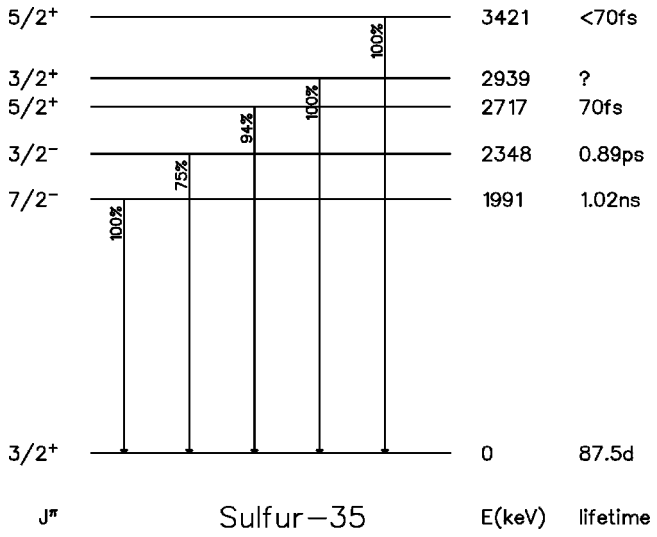

FIG. 1. ^{35}S energy level diagram showing cleanly identified γ-rays. The energies, spin-parities, lifetimes, and branching ratios were taken from Ref. [20].

evidence that the energy of the state is actually about 4023 keV.

C. Line intensities

To determine the γ-ray yields per μCl atom formed, we employed the equation

$$Y_\gamma = \frac{N_\gamma}{N_\mu \epsilon \Delta\Omega(E) f_{\rm iso}} C_{ab} C_{sv}, \tag{1}$$

where N_γ is the number of γ-rays detected, N_μ is the number of lifetime-corrected muon stops, $\epsilon\Delta\Omega(E)$ is the photon acceptance at the appropriate energy, $f_{\rm iso}$ is the μ^- Cl atomic capture fraction, and C_{ab} and C_{sv} are minor correction factors, described below. The γ-ray counts N_γ were obtained from fits with Doppler broadened or Gaussian line shapes (see Sec. III A). The atomic capture fraction $f_{\rm iso}=0.59 \pm 0.04$, i.e., the fraction of muon stops in NaCl that undergo atomic capture on Cl, was taken from Ref. [21].[1] The factors C_{ab} and C_{sv} accounted for photon absorption in the target and self-vetoing by the suppressor (C_{ab} varied from 1.02 to 1.03 and C_{sv} varied from 1.06 to 1.16). They are discussed in detail in Ref. [11].

The resulting γ-ray yields per μCl atom formed are given in Table I. The dominant uncertainties were the measurement uncertainty in the atomic capture fraction of $\pm 7\%$ (see Ref. [21] for details) and the normalization uncertainty in the muonic x-ray calibration of $\pm 15\%$ (see Ref. [11] for details). The statistical uncertainties in N_γ and total uncertainties in C_{ab} and C_{sv} were negligible.

[1]For comparison the Fermi Z-law yields $f_{\rm iso}=0.61$ and the calculation of Vogel *et al.* [24] yields $f_{\rm iso}=0.58$. The earlier experimental work of Knight *et al.* [22] gave $f_{\rm iso}=0.56$ and Zinov *et al.* [23] gave $f_{\rm iso}=0.49$.

D. Cascade feeding

A serious concern in γ-ray studies is cascade feeding into interesting ^{35}S levels from higher-lying levels. If missed, such production of ^{35}S states would distort the interpretation of the measured rates, hyperfine dependences and angular correlations.

Although the comparison between our Na^{35}Cl data and the NNDC Tables [20] gave only five clean γ-ray matches, some γ-peaks were never identified and many ^{35}S states have unknown decays. Therefore we performed a $\gamma-\gamma$ coincidence measurement in order to study the total amount of cascade feeding to ^{35}S levels. Specifically, we determined the counts for interesting γ-ray lines in the HPGe singles spectrum (denoted N_S^γ) and the HPGe$\cdot$NaI coincidence spectrum (denoted N_C^γ), and computed the super-ratio

$$f_c = \frac{N_C^\gamma / N_S^\gamma}{N_C^{\rm Co60} / N_S^{\rm Co60}}. \tag{2}$$

The coincidence fraction f_c reflects the total number of other γ-rays in prompt coincidence with the interesting γ–ray. Note in Eq. (2) the ratio $N_C^{\rm Co60}/N_S^{\rm Co60}$ was obtained by measuring the well known 1.17 and 1.33 MeV coincident γ-rays from a Co-60 source. The ratio $N_C^{\rm Co60}/N_S^{\rm Co60}$ serves to normalize the ratio N_C^γ/N_S^γ. We stress that the approach has limitations: (i) it cannot distinguish feeding via a single-step cascade from a multi-step cascade, and (ii) its interpretation assumes an energy-independent acceptance for the γ-ray detection by the NaI array (the latter assumption is fairly reasonable for γ-ray energies from 0.5 to 3.0 MeV). The method is described in detail in Refs. [11,13].

The measured coincidence fractions f_c for ^{35}S γ-rays are listed in column seven of Table I. For the 1991, 2348 and 2717 keV γ-rays the table shows the presence of considerable feeding from unidentified levels. The comparison of experiment and theory is therefore not warranted in such cases. However for the 2939 and 3421 keV γ-rays the table shows the absence of large amounts of cascade feeding. Therefore we focused our attention on the model-data comparison of the physical observables in the ^{35}Cl$(3/2^+,0) \rightarrow ^{35}S(3/2^+,2939)$ transition and the ^{35}Cl$(3/2^+,0) \rightarrow ^{35}S(5/2^+,3421)$ transition.

E. Capture rates

To convert the γ yields to capture rates we accounted for the γ-ray branching ratios (taken from Ref. [20]) and multiplied by the muon disappearance rate (taken from Ref. [25]). For ^{35}Cl$(3/2^+,0) \rightarrow ^{35}S(3/2^+,2939)$ and ^{35}Cl$(3/2^+,0) \rightarrow ^{35}S(5/2^+,3421)$ the resulting rates and experimental uncertainties are listed in Table II.

Because of the hyperfine effect in the μ^-Cl atom, the experimental capture rates are combinations of hyperfine capture rates (for details see Sec. III F). Assuming an initial statistical population of the two hyperfine states, the hyperfine transition rate of Sec. III F, the published muon disappearance rate of Ref. [25], and a 2.0μs wide μ^-STOP gate, the observed rates Λ in Table II are related to the hyperfine

TABLE II. The measured capture rates and hyperfine dependences for the ^{35}Cl$(3/2^+,0)\rightarrow{}^{35}S(3/2^+,2939)$ transition and the ^{35}Cl$(3/2^+,0)\rightarrow{}^{35}S(5/2^+,3421)$ transition. Note that $\Lambda=0.12\Lambda_+ +0.88\Lambda_-$ (see Sec. III F for details).

$(E,J^\pi)_i$ (keV)	Λ ($\times 10^3$ s^{-1})	Λ_+/Λ_-
$(2939,3/2^+)$	12.2 ± 2.2	0.74 ± 0.17
$(3421,5/2^+)$	11.9 ± 2.2	1.60 ± 0.19

capture rates via $\Lambda=0.12\Lambda_+ +0.88\Lambda_-$. The extraction of the hyperfine capture ratio Λ_+/Λ_- is discussed in the following section.

F. Hyperfine dependences

In a nonzero spin $I\neq0$ target the muonic atom's $1S$ atomic state is split into hyperfine states with $F_+=I+1/2$ and $F_-=I-1/2$. Due to the spin dependence of the weak interaction the capture rates from the hyperfine states are usually different. In certain cases (e.g., ^{35}Cl), during the muonic atom lifetime the upper HF state decays to the lower HF state. Consequently, the time dependence of γ-rays from μ^- capture has the form

$$Ae^{-\Lambda_D t}(1+ke^{-\Lambda_h t}), \tag{3}$$

where Λ_D is the μ^- disappearance rate, Λ_h is the hyperfine transition rate, and k is related to the hyperfine dependence of muon capture via $k=f_+(\Lambda_+/\Lambda_- -1)$. The quantity f_+ is the fractional population of the F_+ state at $t=0$. For a spin-3/2 target and a statistical HF population [26] the factor is $f_+=5/8$. Consequently, if Λ_h is neither too fast nor too slow (i.e., $\Lambda_h\sim\Lambda_D$), the hyperfine dependence of muon capture can be determined from the time spectrum of the γ-rays.

For each γ-ray line its time-binned energy spectra were first fit to appropriate Gaussian or Doppler line shapes in order to determine its time spectrum. The γ-ray time spectra themselves were then fit to a convolution of the theoretical time dependence [Eq. (3)] with the measured HPGe time resolution (Sec. III A). We accounted for the slight distortion of the disappearance rate due to muon pile-up in the Na^{35}Cl target by the method described in Ref. [11] (a 4% effect). Additionally we investigated the sensitivities of Λ_+/Λ_- and Λ_h to the various parameters of the instrumental response and the muon pile-up.

In this analysis we employed the 1991 keV γ-ray time spectrum to determine the hyperfine transition rate Λ_h (since the 1991 keV γ-ray has a very large hyperfine effect). Note, our best fit value of $\Lambda_h=10.1\pm1.0\mu s^{-1}$ for this NaCl experiment and the earlier value of $\Lambda_h=8.1\pm2.2\mu s^{-1}$ for a LiCl experiment [27], are consistent (we are also consistent with the recent experiment of Stocki *et al.* [28]). Also our experimental rate is in reasonable agreement with the predicted rate of $\Lambda_h=8.0\ \mu s^{-1}$ from Ref. [29].

The best fit values for the hyperfine dependences of the 2939 keV line and 3421 keV line are given in Table II (in extracting Λ_+/Λ_- we fixed Λ_h using the 1991 keV γ-ray).

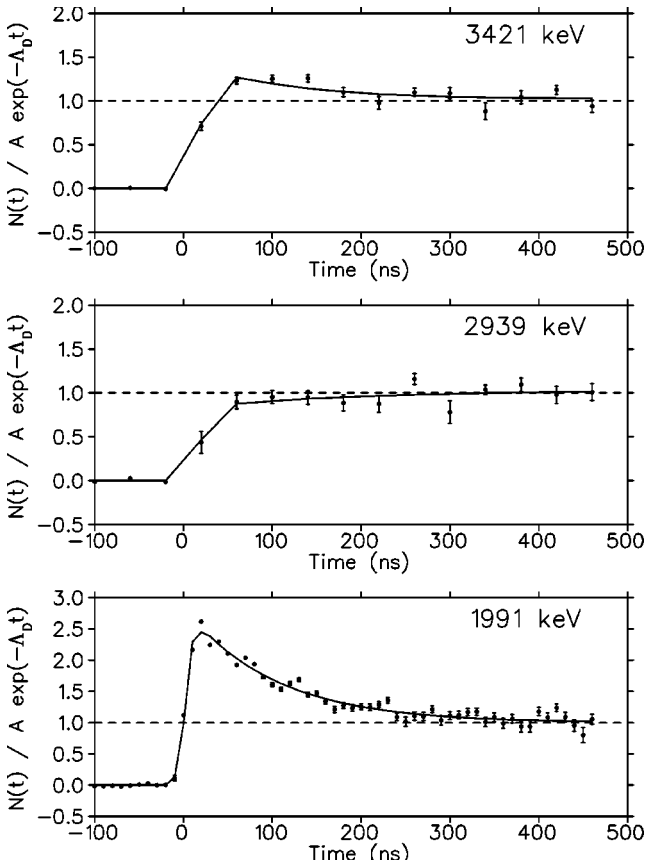

FIG. 2. Time spectra for the 1991 γ-ray (bottom), 2939 γ-ray (center), and 3421 γ-ray (top). The points are the experimental data and the solid lines are the least squares fits. The muon disappearance rate was ''divided out'' to better demonstrate the hyperfine effect. Note the very large hyperfine effect for the 1991 keV γ-ray was used to fix the hyperfine transition rate Λ_h (see Sec. III F for details).

In addition, representative fits to their γ-ray time spectra are shown in Fig. 2 and representative sensitivities to the various fitting parameters are shown in Tables III and IV. The quoted errors for Λ_+/Λ_- include the statistical errors in the fitting procedure and the sensitivities to the determination of the instrumental resolution and the muon pile-up.

G. Angular correlations

Because of the spin dependence of the weak interaction, the recoil produced in muon capture is usually oriented. In general, this recoil orientation yields an angular correlation between the neutrino direction and the decay γ-ray direction. Further, when the γ-decay lifetime is less than the recoil stopping time, the $\gamma-\nu$ directional correlation will be manifest in the γ-ray Doppler spectrum. Both the 2939 keV γ-ray and the 3421 keV γ-ray were Doppler broadened.

For unpolarized muons the directional correlation of the photon and the neutrino has the form

$$1+\alpha P_2(\cos\theta), \tag{4}$$

where θ is the angle between the momentum vectors of the photon and the neutrino, $P_2(\cos\theta)$ is the Legendre polyno-

TABLE III. Results of our studies of the systematic uncertainties in the extraction of the hyperfine dependence for the ^{35}Cl$(3/2^+,0)\rightarrow{}^{35}S(3/2^+,2939)$ transition. The input parameters in the time spectrum fits were the $t=0$ position (t_0), instrumental width (σ), muon disappearance rate (Λ_D), and hyperfine transition rate (Λ_h). The last column is the percentage difference of the hyperfine dependence from its central value. See text for details.

Λ_h $\times 10^6$ s^{-1}	Λ_D $\times 10^6$ s^{-1}	t_0 chans.	σ chans.	k	Λ_+/Λ_-	% diff.
8.0	0.225	1504.04	1.923	-0.15 ± 0.10	0.76 ± 0.16	+2%
10.0	0.225	1504.04	1.923	-0.15 ± 0.10	0.76 ± 0.16	+2%
8.0	0.235	1504.04	1.923	-0.18 ± 0.10	0.71 ± 0.16	−5%
10.0	0.235	1504.04	1.923	-0.19 ± 0.10	0.70 ± 0.16	−6%
10.0	0.225	1503.84	1.923	-0.14 ± 0.10	0.78 ± 0.16	+5%
10.0	0.225	1504.24	1.923	-0.16 ± 0.10	0.74 ± 0.16	0%
10.0	0.225	1504.04	1.82	-0.15 ± 0.10	0.76 ± 0.16	+2%
10.0	0.225	1504.04	2.02	-0.15 ± 0.10	0.76 ± 0.16	+2%
10.0	0.225	1504.04	no tail	-0.15 ± 0.10	0.76 ± 0.16	+2%

mial, and α is the $\gamma-\nu$ angular correlation coefficient. Note, for recoil spins $J\leqslant 2$ or γ-ray multipolarities $L\leqslant 2$, higher-order Legendre polynomials do not contribute.

To fit the γ-ray Doppler spectra, and extract the $\gamma-\nu$ correlation coefficient, we convoluted the theoretical Doppler spectrum with the HPGe instrumental line shape. In the fitting procedure we fixed the line shape parameters at their known values, and studied the background sensitivity by trying background shapes of various forms (e.g., linear, quadratic, and exponential). Representative fits to the 2939 keV and 3421 keV lines are shown in Figs. 3 and 4 and typical sensitivities to the fitting parameters are listed in Tables V and VI. For the 2939 keV line a concern is clearly the background line at 2935 keV, which obscures a portion of the Doppler broadened spectrum of the 2939 keV γ-ray.

Unfortunately the Doppler line shape may be distorted by the slowing down of the recoil ion. Specifically, if the slowing-down time t_s and the γ-ray lifetime τ are comparable, then the line shape is a function of the coefficient α and the ratio τ/t_s. From sample fits with different lifetimes we found the input value of τ/t_s and output value of α were highly correlated when $\tau/t_s>0.05$ (see Figs. 5 and 6). For $\tau/t_s<0.01$ the 2939 keV line yielded $\alpha=-0.43\pm0.13$ and the 2939 keV line yielded $\alpha=-0.39\pm0.05$ (the quoted errors for the coefficients include the statistical uncertainties from the fitting procedure and the various sensitivities to the fitting parameters). However, for $\tau/t_s>0.01$ the magnitude of α decreases as the value of τ/t_s increases. Therefore, since independent determination of the γ-ray lifetimes are currently unavailable, our results for α are functions of τ/t_s (i.e., the plots of Fig. 5 and Fig. 6). When the necessary lifetimes are finally measured the correlation coefficients may be read off these figures.

Finally because of the hyperfine effect, the observed coefficient α is a linear combination of the two coefficients $\alpha_\pm$ of the two $F_\pm$ states. Specifically the observed correlation α is (see Ref. [37] for details)

$$\alpha=\frac{n_+\Lambda_+\alpha_++n_-\Lambda_-\alpha_-}{n_+\Lambda_++n_-\Lambda_-}, \tag{5}$$

TABLE IV. Results of our studies of the systematic uncertainties in the extraction of the hyperfine dependence for the ^{35}Cl$(3/2^+,0)\rightarrow{}^{35}S(5/2^+,3421)$ transition. The input parameters in the time spectrum fits were the $t=0$ position (t_0), instrumental width (σ), muon disappearance rate (Λ_D), and hyperfine transition rate (Λ_h). The last column is the percentage difference of the hyperfine dependence from its central value. See text for details.

Λ_h $\times 10^6$ s^{-1}	Λ_D $\times 10^6$ s^{-1}	t_0 chans.	σ chans.	k	Λ_+/Λ_-	% diff.
8.0	0.225	1504.04	1.923	0.41 ± 0.11	1.66 ± 0.18	+4%
10.0	0.225	1504.04	1.923	0.40 ± 0.10	1.64 ± 0.16	+2%
8.0	0.235	1504.04	1.923	0.35 ± 0.10	1.56 ± 0.18	−3%
10.0	0.235	1504.04	1.923	0.34 ± 0.10	1.54 ± 0.18	−4%
10.0	0.225	1503.84	1.923	0.34 ± 0.10	1.54 ± 0.18	−4%
10.0	0.225	1504.24	1.923	0.37 ± 0.10	1.59 ± 0.18	−1%
10.0	0.225	1504.04	1.82	0.39 ± 0.10	1.62 ± 0.18	+1%
10.0	0.225	1504.04	2.02	0.39 ± 0.10	1.62 ± 0.18	+1%
10.0	0.225	1504.04	no tail	0.38 ± 0.07	1.61 ± 0.11	+1%

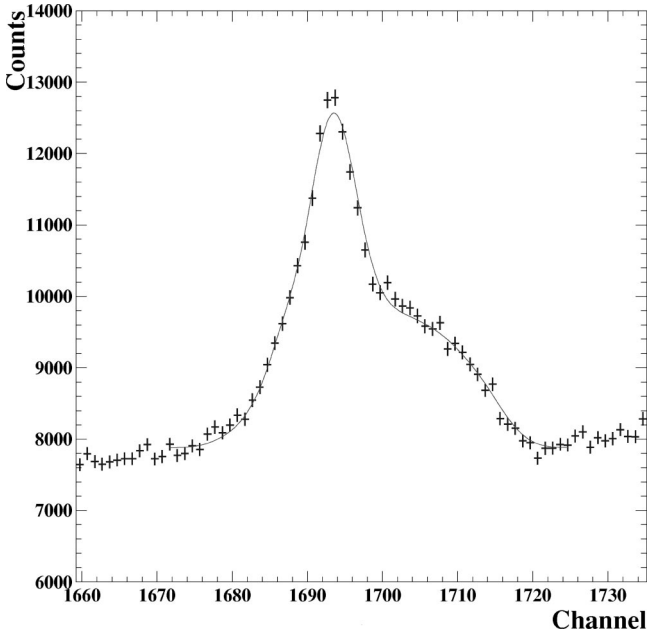

FIG. 3. Sample fit to the Doppler broadened energy spectrum of the 2939 keV γ-ray (the narrower Gaussian-shaped peak is a ^{33}S background line at 2935 keV).

where n_+/n_- is the relative muon occupancy of the hyperfine states and Λ_+/Λ_- is the relative capture rates from the hyperfine states. The relative occupancy was taken from Sec. III F, and is $n_+/n_- = 0.12/0.88 = 0.14$. The hyperfine dependences were taken from Table II, and are 0.74 ± 0.17 for the $(2939,3/2^+)$ transition and 1.60 ± 0.19 for the $(3421,5/2^+)$ transition. This yields $\alpha = 0.09\alpha_+ + 0.91\alpha_-$ for the $(2939,3/2^+)$ transition and $\alpha = 0.18\alpha_+ + 0.82\alpha_-$ for the $(3421,5/2^+)$ transition.

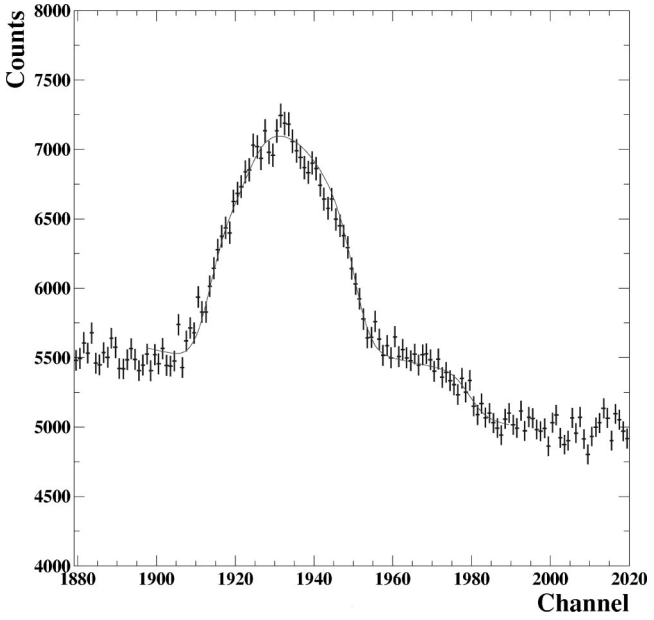

FIG. 4. Sample fit to the Doppler broadened energy spectrum of the 3421 keV γ-ray (the weaker Doppler broadened peak is a ^{23}Ne background line at 3432 keV).

TABLE V. The systematic uncertainties in extracting the $\gamma-\nu$ correlation coefficient from the Doppler lineshape of the $^{35}\mathrm{Cl}(3/2^+,0) \rightarrow {}^{35}\mathrm{S}(3/2^+,2939)$ transition. Note we used a Gaussian instrumental lineshape with a centroid E_0, width σ, and small low-energy tail. Different polynomials of different powers were used to explore the sensitivity to the parametrization of the background (i.e., $\Sigma_i x^i$). The last column is the percentage difference of the angular correlation from its central value. See text for details.

Parameter varied	Amount changed	Correlation α	% diff.
$\Sigma_i x^i$	$i=0.0$	-0.44 ± 0.04	-2%
$\Sigma_i x^i$	$i=1.0$	-0.44 ± 0.04	-2%
$\Sigma_i x^i$	$i=2.0$	-0.44 ± 0.04	-2%
σ	$+20.0\%$	-0.31 ± 0.04	$+28\%$
σ	$+10.0\%$	-0.37 ± 0.04	$+14\%$
σ	-10.0%	-0.49 ± 0.03	-14%
σ	-20.0%	-0.55 ± 0.03	-28%
E_0	$+0.4$ changed	-0.33 ± 0.04	$+23\%$
E_0	$+0.2$ changed	-0.36 ± 0.04	$+16\%$
E_0	-0.2 changed	-0.49 ± 0.04	-14%
E_0	-0.4 changed	-0.54 ± 0.04	-26%
Tail	$+50.0\%$	-0.39 ± 0.03	$+9\%$
Tail	-50.0%	-0.42 ± 0.03	$+2\%$

IV. INTERPRETATION

Herein we discuss the comparison of experiment and theory for the measured observables in the allowed transitions to the $(2939,3/2^+)$ level and the $(3421,5/2^+)$ level. In Sec. IV A we describe the general dependences on weak dynamics, and in Sec. IV B we discuss the model calculation and input parameters. Section IV C compares the model re-

TABLE VI. The systematic uncertainties in extracting the $\gamma-\nu$ correlation coefficient from the Doppler line shape of the $^{35}\mathrm{Cl}(3/2^+,0) \rightarrow {}^{35}\mathrm{S}(5/2^+,3421)$ transition. Note we used a Gaussian instrumental line shape with a centroid E_0, width σ, and small low-energy tail. Different polynomials of different powers were used to explore the sensitivity to the parametrization of the background (i.e., $\Sigma_i x^i$). The last column is the percentage difference of the angular correlation from its central value. See text for details.

Parameter varied	Amount changed	Correlation α	% diff.
$\Sigma_i x^i$	$i=0.0$	-0.39 ± 0.04	0%
$\Sigma_i x^i$	$i=1.0$	-0.38 ± 0.04	$+3\%$
$\Sigma_i x^i$	$i=2.0$	-0.39 ± 0.04	0%
σ	$+20.0\%$	-0.41 ± 0.04	-5%
σ	$+10.0\%$	-0.40 ± 0.04	-3%
σ	-10.0%	-0.39 ± 0.03	0%
σ	-20.0%	-0.39 ± 0.03	0%
E_0	$+0.4$ changed	-0.39 ± 0.04	0%
E_0	$+0.2$ changed	-0.39 ± 0.04	0%
E_0	-0.2 changed	-0.38 ± 0.04	$+3\%$
E_0	-0.4 changed	-0.39 ± 0.04	0%

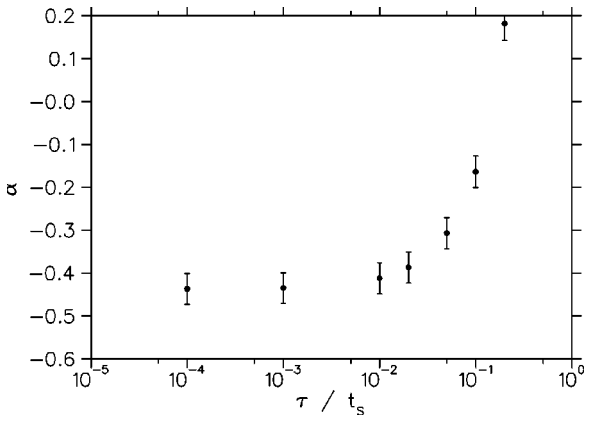

FIG. 5. The γ-ν angular correlation coefficient α versus the ratio τ/t_s for the ^{35}S 2939 keV γ-ray. Only the statistical errors in α are plotted.

sults with the experimental data, and emphasizes the sensitivities to the weak couplings and the nuclear structure.

Note that we restrict the comparison of theory and experiment to the capture rates and the hyperfine dependences. Interpretation of the correlations is not possible at the moment as the γ-decay lifetimes and their mixing ratios are not currently available.

A. Fujii-Primakoff approximation

To demonstrate the basic features of the physical observables in allowed $3/2^+ \rightarrow 3/2^+$ and $3/2^+ \rightarrow 5/2^+$ transitions we first review some results of the Fujii–Primakoff approximation [30,31]. Recall that the Fujii-Primakoff Hamiltonian for nuclear muon capture [32] is

$$H = \tau^+ \frac{1-\sigma\cdot\hat{\nu}}{2}\sum_{i=1}^{A}\tau_i^- \times (G_V 1\cdot 1_i + G_A\ \sigma\cdot\sigma_i + G_P\sigma\cdot\hat{\nu}\sigma_i\cdot\hat{\nu})\,\delta(r-r_i), \tag{6}$$

where $\hat{\nu}$ is the ν-momentum unit vector, 1 and σ are unit and spin matrices (the operators with subscripts act on nucleons and the operators without subscripts act on leptons), and τ^+ converts the muon into a neutrino. Note that the leading contribution of g_a is to the effective coupling G_A and the leading contribution of g_p is to the effective coupling G_P. In the Fujii-Primakoff approximation only the allowed GT operator and the allowed Fermi operator are retained following the multipole expansion of Eq. (6).

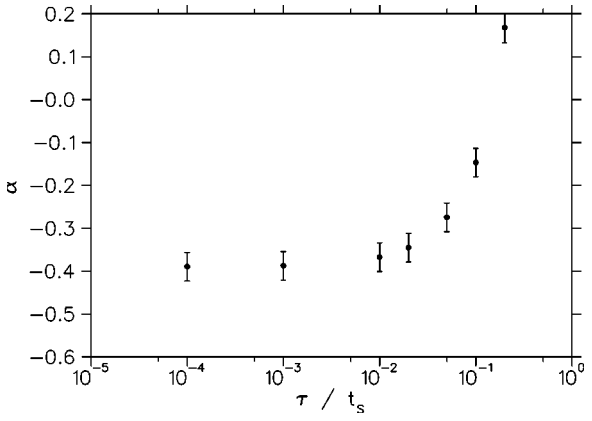

FIG. 6. The γ-ν angular correlation coefficient α versus the ratio τ/t_s for the ^{35}S 3421 keV γ-ray. Only the statistical errors in α are plotted.

First consider the hyperfine dependence of muon capture. We note in the multipole expansion of the Fujii-Primakoff Hamiltonian the G_A term makes allowed contributions to neutrino waves with total angular momentum $j^\pi = 1/2^+$ only whereas the G_P term makes allowed contributions to neutrino waves with total angular momentum $j^\pi = 3/2^+$ [this difference is because of $\hat{\nu}$ in Eq. (6)]. In $3/2^+ \rightarrow 5/2^+$ transitions, neutrinos with $j = 1/2^+$ may be emitted in F_+ capture, but neutrinos with $j = 3/2^+$ must be emitted in F_- capture. This makes $\Lambda_+/\Lambda_- \gg 1$ and a strong function of the ratio g_p/g_a. However in $3/2^+ \rightarrow 3/2^+$ transitions the emission of $j = 1/2^+$ neutrinos is possible for both F_+ atoms and F_- atoms. This makes $\Lambda_+/\Lambda_- \sim 1$ and a weaker function of the ratio g_p/g_a.

Next consider the $\gamma-\nu$ correlation in muon capture. Note in Eq. (6) the G_A term is a vector in spin–space while the G_P term is a scalar in spin–space. Consequently, in most cases the magnetic substates of recoil nuclei are populated differently by allowed contributions that originate from the G_A term and the G_P term. This makes the recoil orientation, and therefore the $\gamma-\nu$ correlation, a function of g_p/g_a. However an exception is $\gamma-\nu$ correlations in $3/2^+ \rightarrow 5/2^+$ transitions on F_- atoms. In such circumstances the emission of d-wave ν's is required and only the G_P term generates an allowed contribution. Consequently for $3/2^+ \rightarrow 5/2^+$ transitions on F_- atoms the recoil orientation and $\gamma-\nu$ correlation is independent of the coupling constants in the Fujii–Primakoff approximation. The potential usefulness of the $\gamma-\nu$ correlation coefficients for model testing is illustrated further in the Appendix.

In summary, different observables offer different sensitivities to the weak couplings and the nuclear structure. For example, the hyperfine dependence Λ_+/Λ_- in a $3/2^+ \rightarrow 5/2^-$ transition is particularly sensitive to the induced pseudoscalar coupling and the correlation coefficient α_- in a $3/2^+ \rightarrow 5/2^-$ transition is particularly sensitive to the forbidden matrix elements. In principle they enable a means of both extracting the weak couplings and testing the nuclear structure.

B. Model calculation

Our model calculations of the capture rates and hyperfine dependences were performed in the impulse approximation using the shell model (equations for the capture rates and the hyperfine dependences are published in Refs. [33,34,37]). Specifically, we used the computer code OXBASH [35], the complete $1s-0d$ space, and the universal SD interaction [36]. We fixed the weak vector and magnetic couplings to the values $g_v = 1.000$ and $g_m = 3.706$ and varied the weak axial and induced pseudoscalar couplings. The $A = 35$ nuclear matrix elements were computed with harmonic oscillator wave

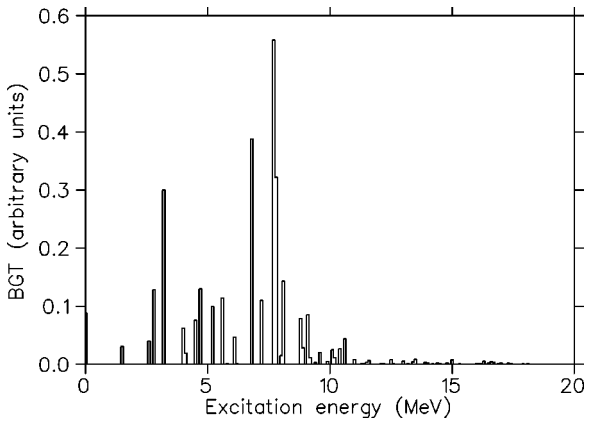

FIG. 7. The calculated distribution of ^{35}Cl$\rightarrow^{35}$S allowed GT strength distribution (B_GT) using the $1s$–$0d$ shell model and the universal SD interaction (see text for details).

functions and an oscillator parameter $b=1.90$ fm. The momentum transfer was computed using the experimental values of excitation energies (giving $q=101.17$ MeV/c for the 2939 keV state and $q=100.59$ MeV/c for the 3421 keV state). Finally the μ^- ^{35}Cl atomic wave function was assumed to be uniform in the nuclear volume and computed employing a muon wavefunction reduction factor of $R=0.521$ (see Walecka [33] and references therein). More details are given in Ref. [11].

The arguments we made in Sec. IV A for sensitivities of observables to g_a and g_p were based on the dominance of the allowed GT matrix element in the interesting (μ,ν) transition. However our model calculations show a large $(0d_{5/2})^{12}(1s_{1/2})^4(0d_{3/2})^3$ component in the ^{35}Cl ground state and a large $(0d_{5/2})^{12}(1s_{1/2})^3(0d_{3/2})^4$ component in the two ^{35}S states. Consequently the $1s_{1/2}\rightarrow 0d_{3/2}$ single particle transition is important in both ^{35}Cl$(3/2^+,0)\rightarrow^{35}S(3/2^+,2939)$ and ^{35}Cl$(3/2^+,0)\rightarrow^{35}S(5/2^+,3421)$. Furthermore for $1s_{1/2}\rightarrow 0d_{3/2}$ single particle transitions the allowed GT matrix element is zero (the operator obeying a $\Delta l=0$ selection rule). This amplifies the importance of $l=2$ forbidden contributions in both transitions. A serious concern is clearly therefore the correct accounting for $l=2$ forbidden contributions from the $1s_{1/2}\rightarrow 0d_{3/2}$ single particle transition in the ^{35}Cl$(3/2^+,0)\rightarrow^{35}S(3/2^+,2939)$ and the ^{35}Cl$(3/2^+,0)\rightarrow^{35}S(5/2^+,3421)$.[2]

We further note that the calculation shows that the ^{35}Cl $\rightarrow^{35}$S GT strength is spread over many states with $E_x<10$ MeV (see Fig. 7). This contrasts with ^{23}Na$\rightarrow^{23}$Ne and ^{28}Si$\rightarrow^{28}$Al (other cases of μ capture work on $1s$–$0d$ nuclei) where only a few states are found to exhaust a large fraction of GT strength (for more details see Gorringe *et al.* [15]).

[2]The full calculation shows numerous other configurations with additional holes in the $0d_{5/2}$–$1s_{3/2}$ orbitals of the relevant $A=35$ states. These generate single particle contributions in ^{35}Cl$(3/2^+,0)\rightarrow^{35}S(3/2^+,2939)$ and ^{35}Cl$(3/2^+,0)\rightarrow^{35}S(5/2^+,3421)$ involving $0d\rightarrow 0d$ and $1s\rightarrow 1s$ transitions. Such single particle transitions generate substantial allowed Gamow–Teller contributions.

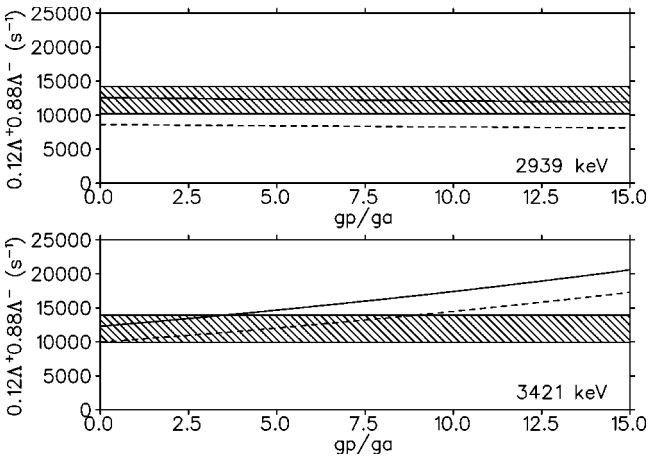

FIG. 8. The calculated capture rate $\Lambda=0.12\Lambda_+ +0.88\Lambda_-$ for the ^{35}Cl$(3/2^+,0)\rightarrow^{35}S(3/2^+,2939)$ transition (top) and the ^{35}Cl$(3/2^+,0)\rightarrow^{35}S(5/2^+,3421)$ transition (bottom). The solid lines are for $g_a=-1.26$ and the dashed lines are for $g_a=-1.00$. The shaded bands correspond to our experimental results.

C. Comparison of experiment and theory

Figure 8 shows the results of our calculations of the capture rate $\Lambda=0.12\Lambda_+ +0.88\Lambda_-$ to the $(2939,3/2^+)$ state and the $(3421,5/2^+)$ state. As expected we found that the rate is most sensitive to the value of the coupling g_a. For $g_a=-1.26$ and $g_p/g_a=6.8$ the computed rates were 12.2×10^3 s^{-1} for the $(2939,3/2^+)$ state and 15.4×10^3 s^{-1} for the $(3421,5/2^+)$ state. For $g_a=-1.00$ and $g_p/g_a=6.8$ the computed rates were 8.4×10^3 s^{-1} for the $(2939,3/2^+)$ state and 12.3×10^3 s^{-1} for the $(3421,5/2^+)$ state. The calculated rates are remarkably close to the corresponding measurements of $(12.2\pm2.2)\times10^3$ s^{-1} and $(11.9\pm2.2)\times10^3$ s^{-1} respectively.

Concerning the induced pseudoscalar coupling, the calculated $(3421,5/2^+)$ rate was found to exhibit some sensitivity to g_p but the calculated $(2939,3/2^+)$ rate was found to exhibit no sensitivity to g_p (see Fig. 8). This finding is in agreement with the expectations of the Fujii–Primakoff approximation (see Sec. IV A).

Figure 9 shows the results of our calculations for the hyperfine dependence Λ_+/Λ_- of the $(2939,3/2^+)$ transition and the $(3421,5/2^+)$ transition. Note as argued in Sec. IV A, the $3/2^+\rightarrow 5/2^+$ hyperfine effect is quite strongly dependent on g_p whereas the $3/2^+\rightarrow 3/2^+$ hyperfine effect is quite weakly dependent on g_p. For $g_p/g_a=6.7$ the calculation gives $\Lambda_+/\Lambda_-=1.3$–1.4 for the $(3421,5/2^+)$ transition and $\Lambda_+/\Lambda_-=0.45$–0.46 for the $(2939,3/2^+)$ transition (the range corresponds to choosing either $g_a=-1.00$ or $g_a=-1.26$). For comparison the experimental values are 1.60 ± 0.19 and 0.74 ± 0.17, respectively.

Clearly the model calculations and experimental results for hyperfine dependences are in semiquantitative agreement; for example, both concurring that F_- capture is stronger for the $(2939,3/2^+)$ transition and F_+ capture is stronger for the $(3421,5/2^+)$ transition. However, at the level of 1–2 σ, some indication of disagreement between model and data

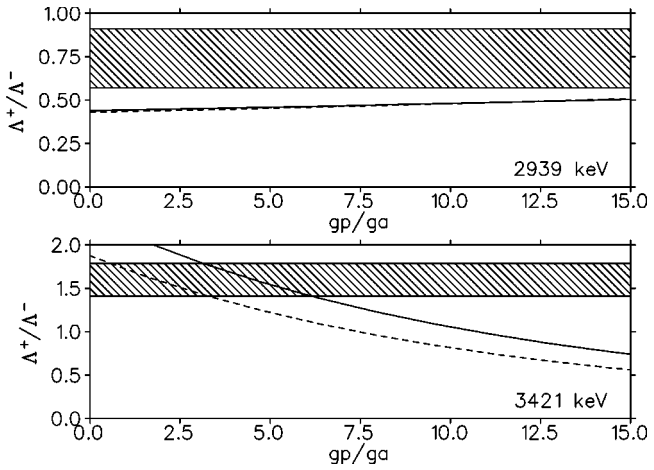

FIG. 9. The hyperfine dependence Λ_+/Λ_- for the ^{35}Cl$(3/2^+,0)\rightarrow{}^{35}S(3/2^+,2939)$ transition (top) and the ^{35}Cl$(3/2^+,0)\rightarrow{}^{35}S(5/2^+,3421)$ transition (bottom). The solid lines are for $g_a=-1.26$ and the dashed lines are for $g_a=-1.00$. The shaded bands correspond to our experimental results.

is suggested for $g_p/g_a=6.7$, the data favoring a smaller value of g_p/g_a.

Is this evidence for the medium modification of the induced coupling? Recall in discussing the $A=35$ structure in Sec. IV B we identified the large contribution of $1s_{1/2}\rightarrow 0d_{3/2}$ transitions and $l=2$ forbidden operators. For example, the fact that $\Lambda_+\sim\Lambda_-$ not $\Lambda_+\gg\Lambda_-$ for ^{35}Cl$(3/2^+,0)\rightarrow{}^{35}S(5/2^+,3421)$, both in the data and in the model, is supporting evidence that forbidden terms are important here. This means that the observables are sensitive to the ratio between the allowed Gamow-Teller matrix elements and the various $l=2$ forbidden matrix elements. The matrix elements are rather dependent on the particular admixtures of the various hole-states in the leading $(0d_{5/2})^{12}(1s_{1/2})^4(0d_{3/2})^3$ configuration for ^{35}Cl and the leading $(0d_{5/2})^{12}(1s_{1/2})^4(0d_{3/2})^3$ configuration for ^{35}S. Therefore we believe it is unwise to blame the coupling g_p for the small discrepancies between the model and the data.

In Sec. III D we discussed in detail our concerns over cascade feeding from the higher lying ^{35}S levels into the interesting ^{35}S levels. Although no higher lying levels were convincingly identified in the singles data, and no γ-ray coincidences were observed in the coincidence data, a contribution of up to 30% feeding to the 2939 keV level and up to 25% feeding to the 3421 keV level is not excluded. For the capture rates the ''worse case scenario'' for cascade feeding would mean the quoted rates for direct capture to interesting levels are overestimated by 25–30 %. In such circumstances the direct rates would still be consistent with the model calculation using $g_a=-1.0$ but would be less consistent with the model calculation using $g_a=-1.25$. For the hyperfine dependences the ''worse case scenario'' for cascade feeding is somewhat more difficult to quantify. For the 2939 keV line a 30% feeding from a higher lying state with a hyperfine dependence $0.06<\Lambda_+/\Lambda_-<1.4$ would not change our result by more than the quoted experimental uncertainty ± 0.17, and for the 3421 keV line a 25% feeding from a higher lying state with a hyperfine dependence $0.8<\Lambda_+/\Lambda_-<2.4$ would also not change our result by more than the quoted experimental uncertainty ± 0.19.[3] In such circumstances our conclusions regarding the comparison of model and data and the values of g_a and g_p are not affected. However, with both 25–30 % cascade feeding and a larger hyperfine effect, the measured hyperfine dependences and direct hyperfine dependences would be significantly different. While the combination of such large cascade feeding with such large hyperfine dependences is not excluded by our data, we think it unlikely.

V. CONCLUSION

In summary, we have measured the γ-ray spectra from muon capture on isotopically enriched Na^{35}Cl. For the ^{35}Cl$(3/2^+,0)\rightarrow{}^{35}S(3/2^+,2939)$ transition and ^{35}Cl$(3/2^+,0)\rightarrow{}^{35}S(5/2^+,3421)$ transition we obtained their capture rates, hyperfine dependences and γ-ν correlation coefficients. Concerning the capture rates and hyperfine dependences the experimental results are in semiquantitative agreement with a large basis shell model calculation using $g_p/g_a=6.7$ and $g_a=-1.00$ (or $g_a=-1.26$). However, we note that large $l=2$ forbidden contribution from large $1s_{1/2}\rightarrow 0d_{3/2}$ single particle transitions are probable indications of model dependences. We therefore are unwilling to claim a determination of g_p nor g_a, with any precision.

For the angular correlations, since independent measurements of γ-ray lifetimes and mixing ratios are currently unavailable, the comparison of model and data was thwarted. With such supplemental γ-ray data the correlation coefficients for the two γ-rays would permit additional testing of the calculation and the extraction of the coupling g_p. For further details see Sec. III G and the Appendix. We therefore encourage any future efforts to measure these quantities.

We would also encourage a more thorough theoretical investigation of these allowed Gamow-Teller transitions. In particular, a more quantitative assessment of the model uncertainties and the various approximations is worthwhile. For example, in our model we have employed a uniform muon wavefunction and harmonic oscillator nuclear wave functions, and the effect of these simplifications on the observables should be studied.

ACKNOWLEDGMENTS

We wish to thank the staff of TRIUMF for their support. In addition we thank both Professor Jules Deutsch and Professor Harold Fearing for helpful discussions, and the National Science Foundation (United States) and the Natural Sciences and Engineering Research Council (Canada) for financial assistance.

[3]Note for the 2939 keV line, where $\Lambda_+/\Lambda_-<1$, feeding from a state with a hyperfine effect $\Lambda_+>\Lambda_-$ is more troublesome whereas for the 3421 keV line, where $\Lambda_+/\Lambda_->1$, feeding from a state with a hyperfine effect $\Lambda_+<\Lambda_-$ is more troublesome.

APPENDIX: USEFULNESS OF THE $\gamma-\nu$ CORRELATIONS

In this appendix we describe the usefulness of the $\gamma-\nu$ correlation coefficients in the testing of the nuclear model calculation. We consider the example of the 3421 keV γ-ray from the $(5/2+,3421)$ excited state. Assuming negligible slowing-down effects the measured $\gamma-\nu$ correlation coefficient was found to be $\alpha=-0.39\pm0.05$.

In our toy model for the $^{35}\mathrm{Cl}(3/2^+,0)\rightarrow{}^{35}\mathrm{S}(5/2^+,3421)\rightarrow{}^{35}\mathrm{S}(3/2^+,0)$ sequence we will assume that the $^{35}\mathrm{S}(5/2^+,3421)$ lifetime is fast enough that slowing-down effects are negligible and that the 3421 keV γ-ray is pure M1 radiation. The purpose of the toy model is to illustrate the potential sensitivities of the correlation α, and the importance of a measurement of the $^{35}\mathrm{S}(5/2^+,3421)$ lifetime and the 3421 keV $E2/M1$ mixing ratio.

According to Ciechanowicz and Oziewicz [37] the $\gamma-\nu$ angular correlation coefficient α may be written as the product

$$\alpha=a_2B_2, \tag{A1}$$

where a_2 is determined by the μ capture process and B_2 is determined by the γ-decay process. We obtained a_2 using the $1s-0d$ shell model with the universal SD interaction as discussed in Sec. IV B. We took $B_2=+0.3741$ from Table I of Ciechanowicz and Oziewicz [37] under the assumption of a pure M1 decay. Note that we computed the two correlations coefficients $\alpha^{\pm}$ for the two hyperfine states $F_{\pm}$ and then combined the values to obtain the observed correlation $\alpha=0.18\alpha_+ +0.82\alpha_-$ (see Sec. III G for details).

TABLE VII. Toy model results for the γ-ν correlation coefficient α in the $^{35}\mathrm{Cl}(3/2^+,0)\rightarrow{}^{35}\mathrm{S}(5/2^+,3421)\rightarrow{}^{35}\mathrm{S}(3/2^+,0)$ sequence. The results labeled "full" corresponds to the complete model calculation and the results labeled "approx" corresponds to a model calculation omitting the second forbidden matrix elements. The quoted values are for $g_a=-1.26$.

g_p	α "full"	α "approx"
0	−0.240	−0.216
−4	−0.236	−0.210
−8	−0.232	−0.203
−12	−0.228	−0.196

Our toy model results are given in Table VII for $g_a=-1.26$. It shows results from the full calculation as well as from a calculation omitting the interesting second forbidden matrix elements. As argued in Sec. IV A the correlation coefficient is rather weakly dependent on the induced coupling g_p but somewhat more dependent on second forbidden terms.

Our measured value $\alpha=-0.35\pm0.05$ and the calculated values $\alpha\simeq-0.23$ are significantly different. Unfortunately in the absence of any experimental data on the state lifetime and the $E2/M1$ mixing ratio it is impossible to know if the discrepancy is a reflection of problems in the model calculation of the muon capture or the invalidity of our model assumptions of fast γ-decay and pure $M1$ radiation. We therefore strongly encourage the measurements of τ and δ for the $^{35}\mathrm{S}(5/2^+,3421)\rightarrow{}^{35}\mathrm{S}(3/2^+,0)$ γ-decay.

[1] M.L. Goldberger and S.B. Treiman, Phys. Rev. **111**, 354 (1958).

[2] V. Bernard, N. Kaiser, and Ulf-G. Meissner, Phys. Rev. D **50**, 6899 (1994).

[3] Harold W. Fearing, Randy Lewis, Nader Mobed, and Stefan Scherer, Phys. Rev. D **56**, 1783 (1997).

[4] J. Delorme, M. Ericson, A. Figureau, and C. Thévenet, Ann. Phys. (N.Y.) **102**, 273 (1976).

[5] J. Delorme and M. Ericson, Phys. Rev. C **49**, 1763 (1994).

[6] M. Rho, Annu. Rev. Nucl. Part. Sci. **34**, 531 (1984).

[7] G. Jonkmans, S. Ahmed, D.S. Armstrong, G. Azuelos, W. Bertl, M. Blecher, C.Q. Chen, P. Depommier, T. von Egidy, T.P. Gorringe, M.D. Hasinoff, R.S. Henderson, J.A. Macdonald, S.C. Macdonald, J-M. Poutissou, R. Poutissou, B.C. Robertson, A. Serna-Angel, G.N. Taylor, D.H. Wright, and N-S. Zhang, Phys. Rev. Lett. **77**, 4512 (1996).

[8] D.H. Wright, S. Ahmad, D.S. Armstrong, G. Azuelos, W. Bertl, M. Blecher, C.Q. Chen, P. Depommier, B.C. Doyle, T. von Egidy, T.P. Gorringe, P. Gumplinger, M.D. Hasinoff, D. Healey, G. Jonkmans, A.J. Larabee, J.A. Macdonald, S.C. McDonald, M. Munro, J.-M. Poutissou, R. Poutssou, B.C. Robertson, D.G. Sample, E. Saettler, C.N. Sigler, G.N. Taylor, and N.S. Zhang, Phys. Rev. C **57**, 373 (1998).

[9] P. Ackerbauer, D.V. Balin, V.M. Baturin, G.A. Beer, W.H. Breunlich, T. Case, K. Crowe, H. Daniel, J. Deutsch, J. Govaerts, Yu.S. Grigorev, F.J. Hartmann, P. Kammel, R. King, B. Lauss, E.M. Maev, V.E. Markushin, J. Marton, M. Muhlbauer, C. Petitjean, Th. Petitjean, G.E. Petrov, R. Prieels, W. Prymas, W. Schott, G.G. Semenchuk, Yu.V. Smirenin, A.A. Vorobov, N.I. Voropaev, and P. Wojciechowski, Phys. Lett. B **417**, 224 (1998).

[10] V. Wiaux, R. Prieels, J. Deutsch, J. Govaerts, V.B. Brudanin, V.G. Egorov, C. Petitjean, and P. Truöl, Phys. Rev. C **65**, 025503 (2002).

[11] B.L. Johnson, T.P. Gorringe, J. Bauer, M.A. Kovash, R. Porter, D.S. Armstrong, M.D. Hasinoff, D.F. Measday, B.A. Moftah, and D.H. Wright, Phys. Rev. C **54**, 2714 (1996).

[12] V. Brudanin, V. Egorov, T. Filipova, A. Kachalkin, V. Kovalenko, A. Salamatin, Yu. Shitov, I. Stekl, S. Vasilev, V. Vorobel, Ts. Vylov, I. Yutlandov, Sh. Zaparov, J. Deutsch, R. Prieels, L. Grenacs, J. Rak, and Ch. Briançon, Nucl. Phys. **A587**, 577 (1995).

[13] B.A. Moftah, E. Gete, D.F. Measday, D.S. Armstrong, J. Bauer, T.P. Gorringe, B.L. Johnson, B. Siebels, and S. Stanislaus, Phys. Lett. B **395**, 157 (1997).

[14] Ch. Briançon, V. Brudanin, J. Deutsch, V. Egorov, T. Filipova, M. Kudoyarov, V. Lobanov, T. Mamedov, A. Pasternak, R. Prieels, A. Salamatin, Yu. Shitov, Ts. Vylov, I. Yutlandov, and

Sh. Zaparov, Nucl. Phys. **A671**, 647 (2000).
[15] T.P. Gorringe, D.S. Armstrong, S. Arole, M. Boleman, E. Gete, V. Kuzmin, B.A. Moftah, R. Sedlar, T.J. Stocki, and T. Tetereva, Phys. Rev. C **60**, 055501 (1999).
[16] D. Kessler, H. Mes, A.C. Thompson, H.L. Anderson, M.S. Dixit, C.K. Hargrove, and R.J. McKee, Phys. Rev. C **11**, 1719 (1975).
[17] F.J. Hartmann, T. von Egidy, R. Bergmann, M. Kleber, H.-J. Pfeiffer, K. Springer, and H. Daniel, Phys. Rev. Lett. **37**, 331 (1976).
[18] P. Vogel, Phys. Rev. A **22**, 1600 (1980).
[19] F.J. Hartmann, R. Bergmann, H. Daniel, H.-J. Pfeiffer, T. von Egidy, and W. Wilhelm, Z. Phys. A **305**, 189 (1982).
[20] R.R. Kinsey, computer code NUDAT, National Nuclear Data Center, Brookhaven National Laboratory, Upton, NY, 1996.
[21] L.F. Mausner, R.A. Naumann, J.A. Monard, and S.N. Kaplan, Phys. Rev. A **15**, 479 (1977).
[22] J.D. Knight, C.J. Orth, M.E. Schillaci, R.A. Naumann, H. Daniel, K. Springer, and H.B. Knowles, Phys. Rev. A **13**, 43 (1976).
[23] V.G. Zinov, A.D. Konin, and A.I. Mukhin, Sov. J. Nucl. Phys. **2**, 613 (1966).
[24] P. Vogel, P. Haff, V. Akylas, and A. Winther, Nucl. Phys. **A254**, 445 (1975).
[25] T. Suzuki, D.F. Measday, and J.P. Roalsvig, Phys. Rev. C **35**, 2212 (1987).
[26] J.G. Congleton, Phys. Rev. A **48**, R12 (1993).
[27] T.P. Gorringe, B.L. Johnson, J. Bauer, M.A. Kovash, R. Porter, P. Gumplinger, M.D. Hasinoff, D.F. Measday, B.A. Moftah, D.S. Armstrong, and D.H. Wright, Phys. Lett. B **309**, 241 (1993).
[28] T.J. Stocki, D.F. Measday, E. Gete, M.A. Saliba, J. Lange, and T.P. Gorringe, Phys. Rev. A **64**, 042505 (2001).
[29] R. Winston, Phys. Rev. **129**, 2766 (1963).
[30] S. Ciechanowicz and Z. Oziewicz, Fortschr. Phys. **32**, 61 (1984).
[31] A. Fujii and H. Primakoff, Nuovo Cimento **12**, 327 (1959).
[32] H. Primakoff, Rev. Mod. Phys. **31**, 802 (1959).
[33] J.D. Walecka, in *Muon Physics*, edited by C.S. Wu and V. Hughes (Academic, New York, 1975).
[34] M. Morita and A. Fujii, Phys. Rev. **118**, 606 (1960).
[35] B.A. Brown, A. Etchegoyen, W.D.M. Rae, and N.S. Godwin, MSUCL Report No. 524, 1986.
[36] B.H. Wildenthal, in *Progress in Particle and Nuclear Physics*, edited by D.H. Wilkinson (Pergamon, Oxford, 1984), Vol. 11.
[37] S. Ciechanowicz and Z. Oziewicz, Fortschr. Phys. **32**, 61 (1984).